

**NORTH-HOLLAND  
PHYSICS  
PUBLISHING**



## **A NEW APPROACH TO EVALUATE THE RESPONSE FUNCTIONS FOR CONICAL AND CYLINDRICAL COLLIMATORS**

**G.E. GIGANTE**

*Dipartimento di Energetica dell'Università di Roma "La Sapienza", via Scarpa 14, 00161 Roma, Italy*

Received 24 February 1988 and in revised form 11 July 1988

A new approach to the evaluation of the conical collimator response function is shown. The basic collimator formulae are reviewed. The collimator response function has been found in a very easy way. An approximate solution has been introduced. Studying the response of a measuring system, the use of this approximation strongly reduces the complexity of the relations to be used; therefore it would provide a useful starting point for a Monte Carlo calculation. The errors introduced are less than 10%. Approximate relations that allow the evaluation of the response of conical and cylindrical collimators to plane and line sources are also given.

*Reprinted from* **NUCLEAR INSTRUMENTS AND METHODS  
IN PHYSICS RESEARCH A**

## A NEW APPROACH TO EVALUATE THE RESPONSE FUNCTIONS FOR CONICAL AND CYLINDRICAL COLLIMATORS

G.E. GIGANTE

*Dipartimento di Energetica dell'Università di Roma "La Sapienza", via Scarpa 14, 00161 Roma, Italy*

Received 24 February 1988 and in revised form 11 July 1988

A new approach to the evaluation of the conical collimator response function is shown. The basic collimator formulae are reviewed. The collimator response function has been found in a very easy way. An approximate solution has been introduced. Studying the response of a measuring system, the use of this approximation strongly reduces the complexity of the relations to be used; therefore it would provide a useful starting point for a Monte Carlo calculation. The errors introduced are less than 10%. Approximate relations that allow the evaluation of the response of conical and cylindrical collimators to plane and line sources are also given.

### 1. Introduction

In the last decade many applications of X- and gamma-ray spectrometric techniques (ST) have been developed for "in field" measurements [1–3].

One of the major problems in ST is the identification of the volume involved in the measurement; this problem is of particular importance for X- and gamma-ray scattering techniques (PST), in which the scattering angle may change from point to point inside the scattering volume [4–6].

Another problem concerning collimation is the evaluation of the geometrical limitations of the measuring system with particular regard to "in vivo" measurements, in order to maximize the response/dose ratio.

In many applications a measuring volume of known shape and efficiency is requested. This can be attained by designing the detector and source collimator in an appropriate manner. The computer simulation of the geometrical response (i.e. a point source response of the measuring system) leads to visualization of the measuring volume.

The response function of the collimator was studied in the 1960s and early 1970s in conjunction with the development of nuclear medicine (scanners and gamma-cameras [7,8]). Several computer codes for simulation of the single and multihole collimator systems were also developed in order to take account of interseptal penetration.

The exact collimator response function was found by Steyn et al. [9]. The equations given by these authors are complex in the formalism and cannot be easily visualized. Studying this problem in connection with the simulation of a PST system for bone mineral determina-

tion, we found that equivalent results can be obtained with simple geometrical considerations and an appropriate formalism. In this way the calculation of the solid angle subtended by a collimated detector is easily evaluated with a substantial reduction in the computation time.

### 2. Definitions

A collimator is usually attached to a source and/or detector in order to reduce the field of view; for simplicity we will speak about detector collimation only. As shown in fig. 1a, the single point response of a detector of area  $D$  is given by the solid angle subtended by the point (P)

$$d\Omega = \frac{1}{(4\pi)} \frac{D \cos(\alpha)}{d^2} = \frac{1}{(4\pi)} \frac{Dz}{(x^2 + z^2)^{3/2}}, \quad (1)$$

where  $d$  and  $\alpha$  are defined according to fig. 1. Eq. (1) is valid only if  $D \ll d^2$ .

If we now attach a collimator to the detector, as shown in figs. 1b and c, we have:

$$\begin{aligned} d\Omega &= \frac{1}{(4\pi)} \frac{A(x, z) \cos(\alpha)}{d^2} \\ &= \frac{1}{(4\pi)} \frac{A(x, z)(z + L)}{(x^2 + (z + L)^2)^{3/2}}, \end{aligned} \quad (2)$$

where  $A$  is the portion of the detector area seen by a point of coordinate  $(x, z)$ ; it can be written as a function of the point coordinates,  $A(x, z)$ .

It is worth noting that these definitions are valid for a conical collimator, in which the entrance hole has a

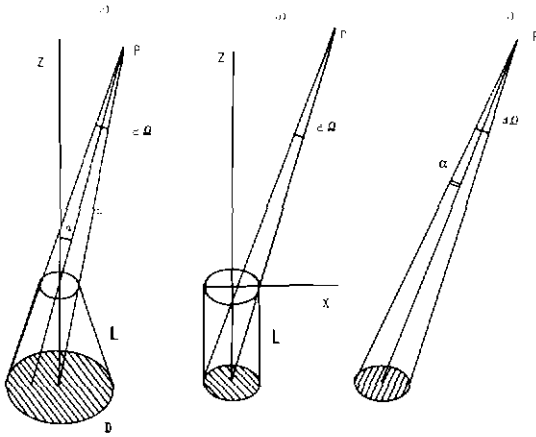


Fig. 1. Solid angle subtended by a detector of area  $D$  without (right) and with a cylindrical (middle) and a conical (left) collimator.

radius  $r'$  different from the detector radius  $r$  (in a cylindrical collimator  $r' = r$ ).

We can now introduce the angle ( $\delta$ ) in connection with the field of view of the detector (fig. 2):

$$\tan(\delta) = \frac{r+r'}{L}, \tag{3}$$

where  $L$  is the height of the collimator.

It is evident that at any height along the collimator axis, the limit of the field of view is given by

$$x_m(z) = r' + \frac{z(r+r')}{L} \tag{4}$$

or

$$x_m(z) = (r'/L)(2z + L), \tag{4'}$$

for a cylindrical collimator.

For a collimator with a conical bore, i.e., divergent from the entrance hole to the detector, we can introduce a focus. In this case the zone of the collimator field of view in which one can see only a portion of the detector area, i.e. the penumbra region, is delimited by an internal cone (see fig. 2). The limit of this cone at any height along the axis  $z$  is given by

$$x_0(z) = r' + \frac{z(r'-r)}{L}. \tag{5}$$

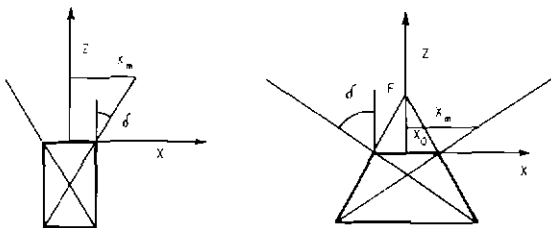


Fig. 2. Definition of divergence angle ( $\delta$ ) and of the upper limit  $x_m$  of the field of view for a cylindrical and conical collimator. For a conical (focusing) collimator  $x_0$  is the low limit of the penumbra region.

If we put  $x_0 = 0$  we find the focus of the collimator

$$F = \frac{Lr'}{r-r'}. \tag{6}$$

### 3. Response function of a collimator

In order to evaluate the response function of a collimator in the case of point, line and plane sources, we should find an expression for the above introduced function  $A(x, z)$ . To this aim let us consider the projection ( $P_r$ ) of the collimator entrance hole on the detector plane; as shown in fig. 3, this projection has always a circular shape with a radius ( $R$ ) that is a function of  $z$ ,  $L$  and  $r'$ :

$$R = [(z + L)/z]r'. \tag{7}$$

It is worth noting that  $R$  becomes larger as we move, along the collimator axis, towards the collimator face (near field), while for large  $z$ -values the radius  $R$  becomes about equal to  $r'$  (far field).

The area  $A$ , which is equal to the detector area for  $x < x_0$ , decreases when we move transversely towards the edge of the field of view. This happens because  $P_r$  moves in the opposite direction. In addition, in fig. 3 is shown how the distance between the centers of  $D$  and  $P_r$  is linearly related to  $x$ :

$$E = (L/z)x. \tag{8}$$

In fig. 4 the area  $A$  is shown in the plane of the detector. In the following, we will show that the area  $A$  can be expressed as a function of  $z$  and of the angles  $\phi$  and  $\gamma$ , as defined according to fig. 4. In addition, we will find a relation between  $x$  and the two above mentioned angles; in this manner we will arrive at an implicit solution of our problem.

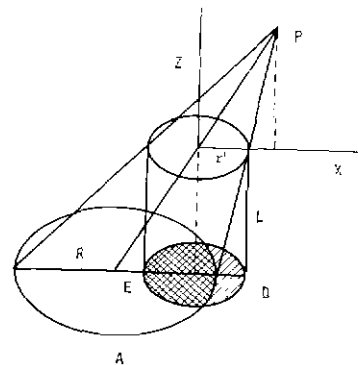


Fig. 3. The area of the detector seen by a point through a cylindrical collimator is given by the intersection of detector area ( $D$ ) and the area ( $P_r$ ) that represents the projection of the collimator entrance hole on the detector plane.

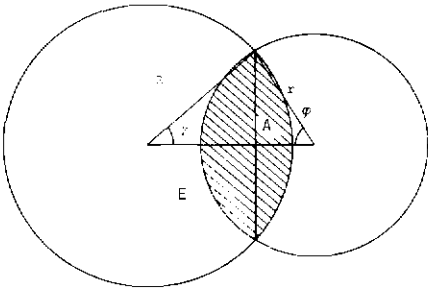


Fig. 4. A view, on the detector plane, of the area  $A(x, z)$  corresponding to the piece of detector area seen by a point through the collimator. The two angles  $\phi$  and  $\gamma$  are defined in the drawing.

It is easy to show that the following relation holds between the angles  $\phi$   $\gamma$ :

$$K = \frac{\sin(\phi)}{\sin(\gamma)} = \frac{R}{r} = \frac{r'(z+L)}{z} \tag{9}$$

or, for a cylindrical collimator:

$$K = \frac{\sin(\phi)}{\sin(\gamma)} = \frac{(z+L)}{z} \tag{9'}$$

It is worth noting that the above defined parameter ( $K$ ) is a function of the collimator height and radius and of the coordinate  $z$ . It assumes values  $\geq 1$ ; for a focusing collimator, if  $z > F$ , this parameter should be substituted by  $K' = r/R$ .

In addition, let us express the distance  $E$  as a function of these two angles, according to fig. 4:

$$E = r \cos(\phi) + R \cos(\gamma) = r[\cos(\phi) + K \cos(\gamma)] \tag{10}$$

$$x = (z/L)[r(\cos(\phi) + K \cos(\gamma))] \tag{10'}$$

It should be noted that when the variable  $\phi$  scans the interval from 0 to 180°, the variable  $\gamma$  scans twice the interval from 0 to  $\arcsin(1/K)$ . In the same time  $E$  varies between  $(R - r)$  and  $(R + r)$ ; this means that its range depends slightly on  $z$ .

Further, we can see that the area  $A$  can be expressed as a function of  $\phi$  and  $\gamma$ , because the intersection area is the sum of two circular segments depending on these angles:

$$A'(\phi, \gamma, z) = r^2 \left[ \phi - \frac{\sin(2\phi)}{2} \right] + R^2 \left[ \gamma - \frac{\sin(2\gamma)}{2} \right],$$

$$\frac{A'(\phi, \gamma, z)}{r^2} = \left[ \phi - \frac{\sin(2\phi)}{2} \right] + K^2 \left[ \gamma - \frac{\sin(2\gamma)}{2} \right]. \tag{11}$$

If  $K = 1$ , i.e. in the focus of the collimator, we find the following simple relation:

$$A'(\phi, \gamma, F)/r^2 = 2\phi - \sin(2\phi) \quad \text{for } 0 \leq \phi \leq (\pi/2). \tag{11'}$$

For  $z > F$ , eq. (11) is still valid but  $R < r$ , therefore the maximum detector area that can be seen is  $\pi R^2$ . Therefore, the angle  $\gamma$  scans the interval 0–180°, whereas  $\phi$  scans twice the interval 0– $\arcsin(1/K')$ . In this case the area  $A$  is given by

$$\frac{A'(\phi, \gamma, z)}{R^2} = K'^2 \left( \phi - \frac{\sin(2\phi)}{2} \right) + \left( \gamma - \frac{\sin(2\gamma)}{2} \right). \tag{12}$$

In fig. 5, a plot of  $A'(\phi, \gamma, z)/r^2$  as a function of  $\phi$  for different values of the parameter  $K$  is shown.

Let us now introduce a normalized coordinate  $x'$  that varies in the interval 0–1 when  $x$  scans the interval  $x_0 - x_m$ . We have:

$$x' = \frac{(x - x_0)}{(x_m - x_0)} = \cos^2(\phi/2) - K \sin^2(\gamma/2), \tag{13}$$

or, for  $K = 1$ ,

$$x' = \cos(\phi).$$

In fig. 6, a plot of  $A/(\pi r^2 d^2)$  vs  $x'$  is shown for different values of  $K$ ; the numerical values are reported in table 1. It is evident that a linear approximation would give quite good results in the range  $0 < x < 0.5$ . We can express this linear approximation as follows:

$$\frac{A(x, z)}{\pi r^2} = f(x') = -x' + 1 = -\frac{(x - x_0)}{(x_m - x_0)} + 1. \tag{14}$$

It is worth noting that the function  $f(x', z)$  overestimates the area  $A$  for large values of  $z$ , i.e. for  $K \approx 1$ . As shown in table 2, the error introduced by this approximation is lower for  $x' < 0.5$ , while for larger  $x'$  (i.e. in the tail of the collimator response function) it is always less than 12% of the full area. Where the errors

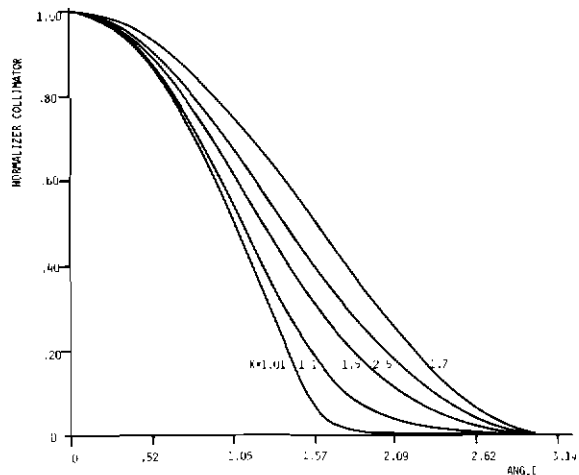


Fig. 5.  $A(\phi, \gamma)/r^2$  as a function of the angle  $\phi$  for some values of the parameter  $K$ .

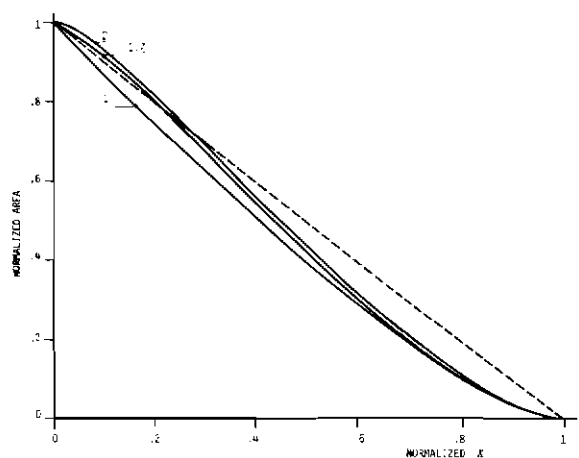


Fig. 6.  $[A(x', z)/(\pi r^2)]$  vs  $x'$  for some values of the parameter  $K$ .

Table 1

Detector area fractions as a function of point normalized coordinate  $x'$  (see eq. (13)), at different values of the parameter  $K$  (see eq. (9))

$x'$	$K$					
	3	2	1.7	1.3	1.1	1
0.1	0.93	0.93	0.92	0.90	0.88	0.87
0.2	0.83	0.82	0.81	0.79	0.76	0.74
0.3	0.72	0.7	0.69	0.66	0.64	0.62
0.4	0.59	0.58	0.56	0.53	0.51	0.5
0.5	0.46	0.44	0.43	0.41	0.4	0.39
0.6	0.34	0.32	0.31	0.3	0.29	0.28
0.7	0.23	0.22	0.21	0.2	0.19	0.18
0.8	0.13	0.12	0.11	0.11	0.11	0.1
0.9	0.05	0.04	0.04	0.04	0.04	0.03

Table 2

Percentage differences of the detector area fractions, calculated with the linear approximation of eq. (14) and with eq. (11), as a function of normalized coordinate  $x'$  (eq. (13)) and of the parameter  $K$  (see eq. (9))

$x'$	$K$					
	3	2	1.7	1.3	1.1	1
0.1	3	3	2	-	-2	-3
0.2	3	2	1	-1	-4	-6
0.3	2	-	-1	-4	-6	-8
0.4	-1	-2	-4	-7	-9	-10
0.5	-4	-6	-7	-9	-10	-11
0.6	-6	-8	-9	-10	-11	-12
0.7	-7	-8	-9	-10	-11	-12
0.8	-7	-8	-9	-9	-9	-10
0.9	-5	-6	-6	-6	-6	-7

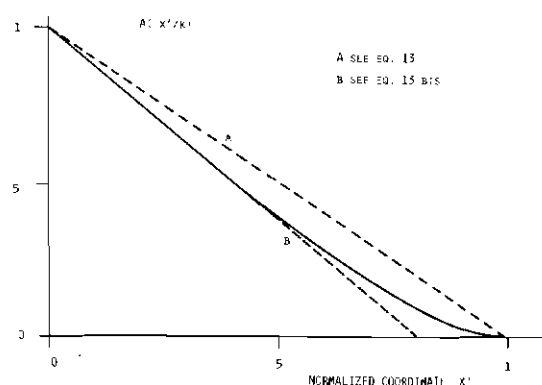


Fig. 7. The linear approximations introduced in eqs. (14) and (14') are reported. For comparison the plot of  $A(x')$  calculated using eqs. (11') and (13) is shown.

are larger, i.e. if  $K \approx 1$ , a better linear approximation can be introduced that underestimates the area  $A$  at larger  $x'$  values:

$$\begin{aligned} \frac{A(x, z)}{\pi r^2} &\approx g(x') = -1.25x' + 1 \\ &= -1.25 \frac{(x - x_0)}{(x_m - x_0)} + 1. \end{aligned} \quad (14')$$

In fig. 7 plots of the two functions  $f(x')$ , curve A, and  $g(x')$ , curve B, are shown; for comparison a plot of  $A/(\pi r^2)$  vs  $x'$  for  $K = 1$ , curve C, is shown.

Finally, the single point response can be calculated combining eqs. (11) or (12) and (2). For a measuring system of more than one collimator the point source response is given by the product of the solid angles subtended by the point in the direction of each collimator. For example, in a system in which both the detector and the source are collimated, the point source response is given by the product of the two solid angles subtended respectively.

#### 4. Response function to a plane and a line source

The plane source response ( $G$ ) is the integral over the plane of the function  $\Omega(x, y, z)$ . If we consider a plane source of radius  $x$  normal to the collimator axis, and we use the linear approximation introduced in the previous section, we can find an approximate formula as shown in appendix 1. The result given in eq. (15) slightly overestimates the plane response:

$$\begin{aligned} G &= \frac{\pi r^2}{2} \left\{ 1 + \frac{(z + L)}{(x_m - x_0)} \right. \\ &\quad \left. \times \left[ \frac{(x - x_m)}{R(x)} - 2.3 \log \left[ \frac{(x + R(x))}{(x_0 + R(x_0))} \right] \right] \right\}, \end{aligned} \quad (15)$$

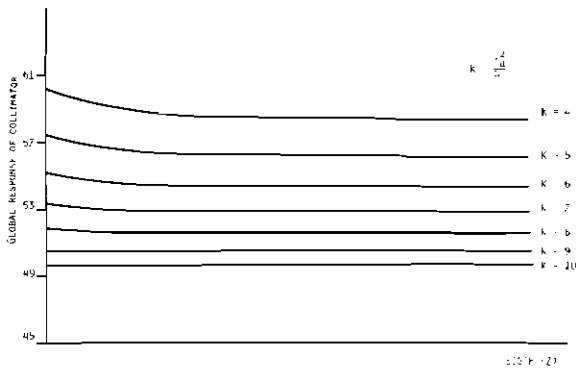


Fig. 8. Response of a plane source as a function of height for some values of  $r^2/L$ . We note that the response to a plane source is almost constant with height.

where  $R(x, z) = [x^2 + (z + L)^2]^{1/2}$  and  $(x_m - x_0) = [(2zr)/L]$ .

Using a well known relation that gives the collimator response to a plane source in the focus [10], it can be easily shown that eq. (15) gives good results if we substitute the second term by 2.3.

For a plane source of infinite size, i.e. when  $x \geq x_m$ , one term in eq. (15) becomes equal to zero and we obtain a simpler relation:

$$G = \frac{\pi r^2}{2} \left\{ 1 - \frac{2.3(z+L)}{(x_m - x_0)} \log \left[ \frac{(x_m + R(x_m))}{(x_0 + R(x_0))} \right] \right\}. \quad (15')$$

Fig. 8 shows a plot of  $G$  vs  $z$  for different values of  $r^2/L$ , for a plane source of infinite size. In agreement with the results of other authors fig. 8 indicates little dependence of  $G$  on  $z$  when the plane source completely fills the field of view of the collimator [11].

The line source response  $T$  can be obtained integrating the function  $\Omega(x, z)$  over a line. In appendix 2 we show that it is possible to find an approximate formula for a line source of length  $x$  using the proposed linear approximation. Using the symbols introduced in eq. (15), it is possible to derive the follow equation:

$$T = \frac{rL}{8z(z+L)^2} \left[ \frac{(x_m x + (z+L)^2)}{R(x)} - R(x_0) \right]. \quad (17)$$

When  $x \geq x_m$  eq. (17) becomes

$$T = \frac{rL}{8z(z+L)^2} [R(x_m) - R(x_0)]. \quad (17')$$

## 5. Discussion

In this paper a simplified representation of a conical collimator response function for point, line and plane

sources is reported. It is shown that a very intuitive solution of the problem can be derived using a simple geometrical approach. In addition, a linear approximation can be used that slightly overestimates the solid angle subtended by the collimator. This approximation can be used to evaluate the scattering volume. This approach has been successfully used by the authors to visualize the scattering volume at different scattering angles.

A simplified formula for the evaluation of single point response in collimated systems is of interest in view of the development of new spectrometers for in situ applications including X-ray fluorescence. When we must take into account attenuation and multiple interaction effects, in conjunction with geometrical problems, the only possibility to evaluate the device performance is to use a Monte Carlo approach. In this case the use of a convenient approximate formula reduces the computation time. Further, when a large sample is used, contributions of geometrical effects become large especially in the presence of low-Z matrices, as in the case of medical applications.

## Acknowledgement

The author wishes to thank Prof. S. Sciuti for his continuous support and for his critical reading of the text.

## Appendix 1

Let us introduce the function

$$R(x, (z+L)) = [x^2 + (z+L)^2]^{1/2}, \quad (18)$$

which gives the distance of any point (P) from the detector center.

In addition, let us introduce the parameter  $B$  given by:

$$B = \frac{1}{(x_m - x_0)}. \quad (19)$$

In the case the response to a plane source is given by:

$$G = \frac{[\pi r^2(z+L)]}{2} \int_0^x \frac{x \, dx}{R^3(x)} + x_0 B \int_{x_0}^x \frac{x \, dx}{R^3(x)} - B \int_{x_0}^x \frac{x^2 \, dx}{R^3(x)}. \quad (20)$$

The three integrals are easily evaluated:

$$\begin{aligned}
 I_1 &= \int_0^x \frac{x \, dx}{R^3(x)} = [(z+L)^{-1} - R(x)^{-1}], \\
 I_2 &= \int_{x_0}^x \frac{x \, dx}{R^3(x)} = [R(x_0)^{-1} - R(x)^{-1}], \\
 I_3 &= \int_{x_0}^x \frac{x^2 \, dx}{R^3(x)} \\
 &= \left[ \frac{x_0}{R(x_m)} - \frac{x}{R(x_0)} \right] - 2 \log \left[ \frac{x + R(x)}{x_0 + R(x_0)} \right].
 \end{aligned} \tag{21}$$

Regrouping the terms, it is possible to derive eq. (15).

## Appendix 2

Let us use the symbols introduced in appendix 1. The line source response is given by:

$$\begin{aligned}
 T &= \frac{[\pi r^2(z+L)]}{2} \int_0^x \frac{dx}{R^3(x)} + xB \int_{x_0}^x \frac{dx}{R^3(x)} \\
 &\quad - B \int_{x_0}^x \frac{x \, dx}{R^3(x)}.
 \end{aligned} \tag{22}$$

The three integrals are easily evaluated:

$$\begin{aligned}
 I_1 &= \int_0^x \frac{dx}{R^3(x)} = \frac{x_m}{(z+L)^2 R(x)}, \\
 I_2 &= \int_{x_0}^x \frac{dx}{R^3(x)} = \frac{1}{(z+L)} \left[ \frac{x_m}{R(x)} - \frac{x_0}{R(x_0)} \right], \\
 I_3 &= \int_{x_0}^x \frac{x \, dx}{R^3(x)} = [R(x_0)^{-1} - R(x)^{-1}].
 \end{aligned} \tag{23}$$

Again, by regrouping the terms and using the definition of the function  $R(x, (z+L))$  given in appendix 1, we can derive eq. (17).

## References

- [1] L.J. Somarville, D.R. Chettle and M.C. Scott, *Phys. Med. Biol.* 9 (1985) 929.
- [2] E. Gatti, P. Rehak and J. Kemmer, *IEEE Trans. Med. Imaging MI-5* (1986) 207.
- [3] G. Harding, J. Kosanetzky and U. Neitzel, *Med. Phys.* 14 (1987) 515.
- [4] B.W. Loo, F.S. Goulding and D.S. Simon, *IEEE Trans. Nucl. Sci. NS-33* (1986) 531.
- [5] A.L. Huddleston, D. Bhaduri and J. Weaver, *Med. Phys.* 6 (1979) 519.
- [6] S.S. Ling, S. Rustgi, A. Karellas, J.D. Craven, J.S. Whiting, M.A. Greenfield and R. Stern, *Med. Phys.* 9 (1982) 208.
- [7] W.J. Mac Intyre, S.O. Fedoruk, C.C. Harris, D.E. Kuhl and J.R. Mallard, in: *Medical Radioisotope Scintigraphy* (IAEA, Vienna, 1969) vol. 1, p. 391.
- [8] G.J. Hine and J.J. Erickson, in: *Instrumentation in Nuclear Medicine*, eds. Hine and Sorenson (Academic Press, New York, 1974).
- [9] J.J. Steyn, D.G. Andrews and M. Dixmier, *Nucl. Instr. and Meth.* 74 (1969) 123.
- [10] R. Di Paola and C. Berche, in: *Traité de Médecine Nucléaire*, eds. G. Meyniel et al. (Flammarion, Paris, 1975).
- [11] R.N. Beck, in: *Medical Radioisotope Scanning* (IAEA, Vienna, 1964) vol. 1, p. 35.